Available online at www.sciencedirect.com
ScienceDirect
Bioorganic & Medicinal Chemistry Letters 16 (2006) 4772–4776
Bioorganic & Medicinal Chemistry Letters

Binding mode of new (thio)hydantoin inhibitors of fatty acid amide hydrolase: Comparison with two original compounds, OL-92 and JP104

Catherine Michaux,[a,b,*] Giulio G. Muccioli,[a,c] Didier M. Lambert[a,c] and Johan Wouters[a,b]

[a]*Drug Design and Discovery Center, FUNDP, 61 rue de Bruxelles, B-5000 Namur, Belgium*
[b]*Laboratoire de Chimie Biologique Structurale, FUNDP, 61 rue de Bruxelles, B-5000 Namur, Belgium*
[c]*Unité de Chimie pharmaceutique et de Radiopharmacie, Ecole de Pharmacie, Faculté de Medecine, UCL, Avenue E. Mounier 73, UCL-CMFA 7340, B-1200 Brussels, Belgium*

Received 9 May 2006; revised 29 June 2006; accepted 29 June 2006
Available online 17 July 2006

Abstract—Substituted (thio)hydantoins (2-thioxoimidazolidinones and imidazolidinediones) were reported as new potential reversible inhibitors of fatty acid amide hydrolase (FAAH). Their binding mode to FAAH was explored to rationalize their activity and give idea to design highly active inhibitors. Starting from the crystal structure of one of these molecules, docking studies provide us with rational basis for the design of new inhibitors within the thiohydantoin family.

Fatty acid amide hydrolase (FAAH) is a membrane enzyme, responsible for the hydrolysis of signaling lipids, including endocannabinoids like anandamide and 2-arachidonoylglycerol.[1–3] FAAH rat isoform was crystallized[4] and is the only characterized mammalian member of the amidase signature superfamily of serine hydrolase bearing a unique catalytic mechanism (Ser-Ser-Lys).[5,6] Anandamide exhibits a range of biological properties having clinical implications in the treatment of sleep disorders, anxiety, epilepsy, cancer, and neurodegenerative disorders.[7–9] Inhibition of FAAH is therefore an interesting and very promising therapeutic target.[10] Some FAAH inhibitors have already been disclosed.[11] These include a series of reversible (e.g., arachidonoyl trifluoromethyl ketone)[12] and irreversible inhibitors (e.g., phenyl methylsulfonyl fluoride[13] or methyl arachidonyl fluorophosphonate (MAFP)[14]). More recently, two classes were identified: a series of irreversible aryl carbamates (e.g., URB597,[15] JP104[16]) and reversible α-ketoheterocycle-based inhibitors (OL-92).[17] In our group, (thio)hydantoins (2-thioxoimidazolidinones and imidazolidinediones) were identified as potential reversible and competitive FAAH inhibitors, devoid of affinity for the cannabinoid receptors.[18] In order to understand the structure–activity relationships (SAR) of this series, characterize their binding mode in the FAAH, and propose potentially more active analogues, structural studies were performed on five selected compounds (Fig. 1).

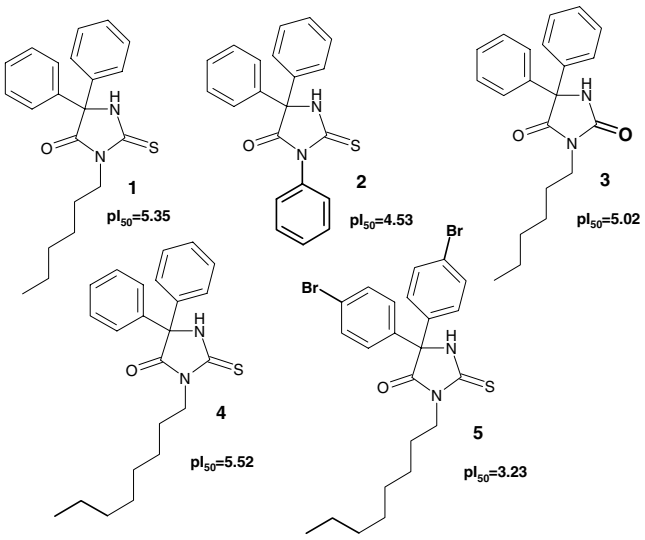

Figure 1. Chemical structure of selected (thio)hydantoin compounds with their inhibitory potency[18] ($pI_{50} = -\log IC_{50}$, obtained using rat brain homogenates and [^{3}H]-anandamide).

Keywords: FAAH; Molecular modeling; (thio)Hydantoin; Crystallography; Binding mode.
* Corresponding author. Tel: +32 0 81724549; fax: +32 0 81724530; e-mail: catherine.michaux@fundp.ac.be

0960-894X/$ - see front matter © 2006 Elsevier Ltd. All rights reserved.
doi:10.1016/j.bmcl.2006.06.087

*Crystal structure of compound **1**.*

Crystal structure determination of **1** (Fig. 2) was carried out in order to elucidate its structural properties, the potential functional groups interacting with the target, and give a stable conformation useful for docking studies.[19] Both phenyl groups are orthogonal and the alkyl chain is stabilized in an extended conformation. Intramolecular C15H···O1 bond restraints the orientation of phenyl groups. In the crystal packing, H bond, CH···π and π–π interactions are observed and can influence the binding to the enzyme.

Binding mode of (thio)hydantoins by docking studies. Active site of the rat FAAH (rFAAH) is formed by a hydrophobic tunnel, called the acyl chain binding channel (ACB), leading from the membrane-bound surface to the hydrophilic catalytic triad (Ser241, Ser217, and Lys142). From the membrane, the ACB bifurcates into a lipophilic bulge. A second tunnel, the cytoplasmic access channel (CA), is exposed to the solvent and emerges at about 80° angle from the ACB.[4] The crystal structure of rFAAH in complex with MAFP[4] being the only reported structure of the enzyme was chosen as target for the docking studies even though MAFP is covalently bound to the enzyme (PDB code: 1MT5). MAFP atoms were removed and hydrogens were added to the protein (pH 7.4). As shown in Figure 3, the proposed binding mode of **1** (with the highest fitness score of GOLD, i.e., 56.96, and the best ligand–enzyme complementarities) shows that the alkyl chain replaces the one of MAFP in the ACB. One of the phenyl rings of **1** points toward the catalytic triad. Here the thiohydantoin moiety would play the role of the double bonds of MAFP to correctly orientate the phenyl (nonlinearly curved shape). The other phenyl group fills a lipophilic pocket (Ile491, Phe194, Leu404, Leu192, Gly485, and Leu401) unoccupied by the irreversible inhibitor. The 2-thioxo group points just above Phe381. Such contact is also observed in the crystal packing of **1**. It is important to note that no binding mode where the hydantoin moiety carbonyl interacts with the catalytic triad was proposed since the conformation of the molecule does not allow it.

To test the proposed binding mode, less and more active analogues of **1**, compounds **2**–**5** (Fig. 1), were also docked in rFAAH. The general binding mode is the same as **1**. For **2**, both phenyl rings occupy the same

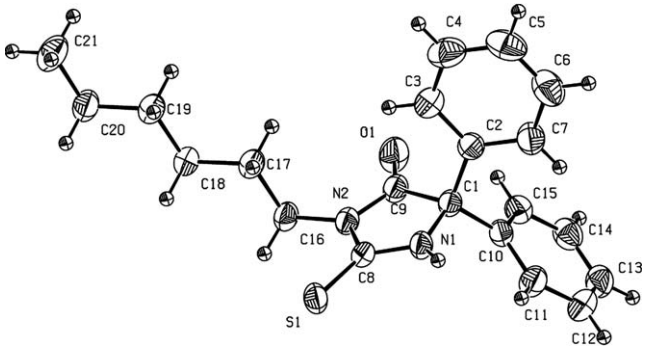

Figure 2. ORTEP view of **1** (50% probability level).

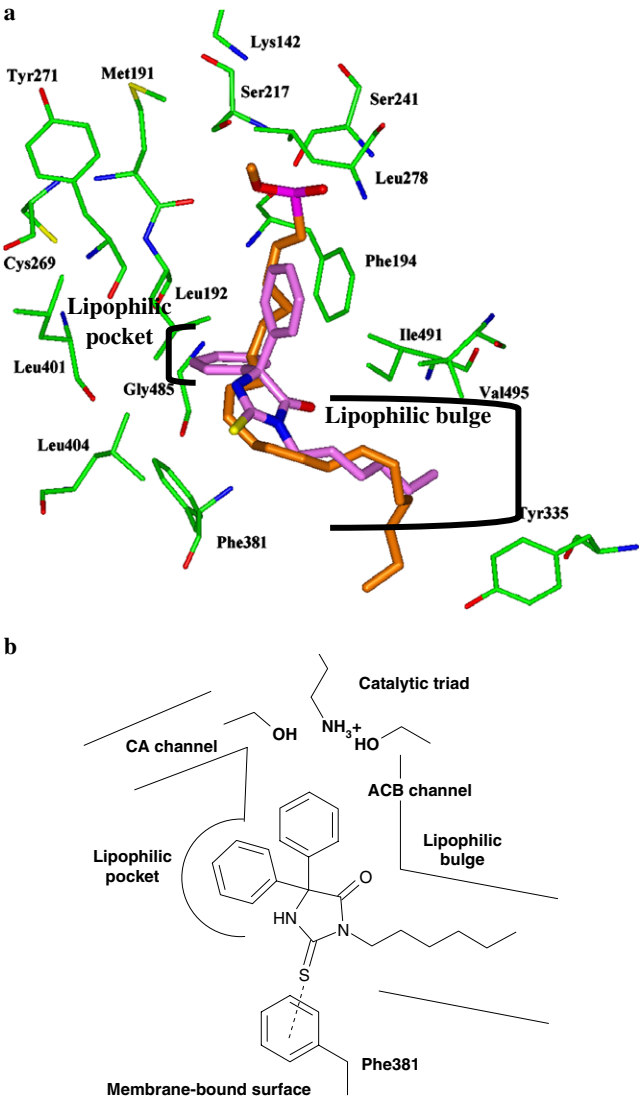

Figure 3. Proposed binding mode of **1** (pink) (a) in the active site of rFAAH, superimposed with the co-crystallized irreversible inhibitor MAFP (orange); (b) in the schematic active site of rFAAH.

pocket as **1** but the hydrophobic bulge is no more filled because the additional N-substituting phenyl rather interacts with Phe381 (π–π interaction), flipping the thiohydantoin moiety by 180°. Essential hydrophobic interactions are therefore probably lost. Compound **4** is more active than **1** because the two additional carbons of the alkyl chain can better occupy the hydrophobic bulge where there is enough space to accommodate longer chains.

Calculated interaction energy is in accordance with the inhibitory potency (Table 1), with the exception of **3** and **5**. In the case of **3**, molecular mechanics cannot reproduce the subtle difference between CO and CS groups. Quantum mechanics was therefore used to explain the better activity of **1** compared to **3**.

Molecular electrostatic potential (mep) maps of the 2-thioxoimidazolidinone and imidazolidinedione moieties were calculated and showed significant differences

Table 1. pI_{50} and interaction energy for compounds **1–5**

Compound	pI_{50}	Interaction energy[a] (kcal/mol)
1	5.35 ± 0.02	−32.8
2	4.53 ± 0.18	−26.4
3	5.02 ± 0.02	−33.0
4	5.52 ± 0.02	−35.8
5	3.23 ± 0.11	−29.0

[a] Interaction energy is the sum of columbic and VdW interactions.

(Fig. 4). The negative zone around CS is less attractive than the one around CO (−44.5 and −55 kcal/mol, respectively) due to a smaller charge on the sulfur atom. If we compare these maps with the one of a benzyl group (mimicking Phe381 interacting with CO and CS), we easily understand why CS is more prone to favorably interact with Phe381 than CO. Even though CS mainly interacts with the CH of a phenyl group, as shown in Figure 5a (data from CSD databank, deduced from Isostar program[20]), CS···π bonds like the one between the thiohydantoin and Phe381 are also observed (pink phenyl in Fig. 5a).

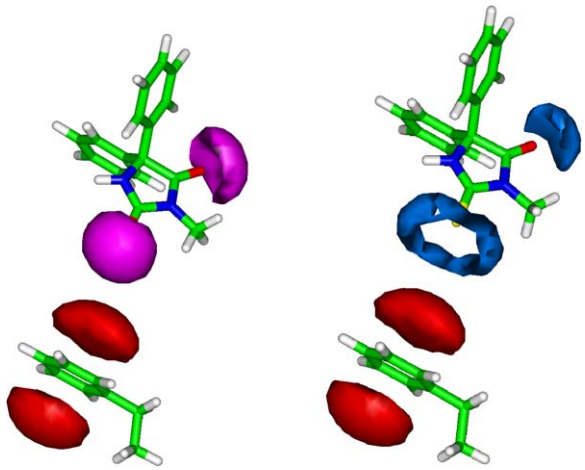

Figure 4. Mep maps of imidazolidinedione moieties (magenta, −30 kcal/mol) and 2-thioxoimidazolidinone (blue; −30 kcal/mol), in comparison with the map of a benzyl group mimicking Phe381 (red, −10 kcal/mol).

In the case of **5**, one of the bromine atoms has unfavorable clashes with the size-limited lipophilic pocket, flipping the phenyl group by 90° and destabilizing the interaction energy. In addition, the electronegative part of bromine atom, highlighted in the mep map (Fig. 5b), faces the carbonyl of Gly485 and Leu401. Such repulsive interaction is probably not correctly modeled thus explaining the discrepancy between the pI_{50} and the energy of interaction. All the results show the reliability of the proposed binding mode which is in accordance with SAR data.

Toward more active compounds.

Reference inhibitors, like JP104 and OL-92, depicted in Figure 6 were also docked in the rFAAH and compared with our new inhibitors. The binding mode observed in GOLD for JP104 and OL-92 is in accordance with the one proposed in the literature.[16,17] Both compounds were noncovalently docked to highlight the initial molecular recognition between the inhibitor and the enzyme. The saturated chain ended by an alkyne or a phenyl group in JP104 and OL-92, respectively, binds the same pocket as the phenyl and alkyl chain of **1** (Fig. 7). In the case of OL-92 and like **1**, the phenyl group can also occupy the lipophilic pocket. The carbamate or the carbonyl group lies near the hydrophilic catalytic triad, forming H bonds, and the biaryl substituents or the keto heterocycle is in the cytoplasmic access (CA) channel, unoccupied by **1**. Interaction energies of both compounds are better than **1** (−36.6 and −40.9 kcal/mol for OL-92 and JP104, respectively), reflecting the higher activity of the compounds, therefore further validating the proposed docking model. As a result, the new 2-thioxoimidazolidinone inhibitors and the reference ones bind to common (i.e., lipophilic bulge and lipophilic pocket) and different pockets (i.e., CA channel). In order to enhance the inhibitory potency of **1**, polar groups, like a carbonyl or an amide moiety, could be *para*-substituted to the phenyl to gain interactions with the hydrophilic catalytic triad (Fig. 8).

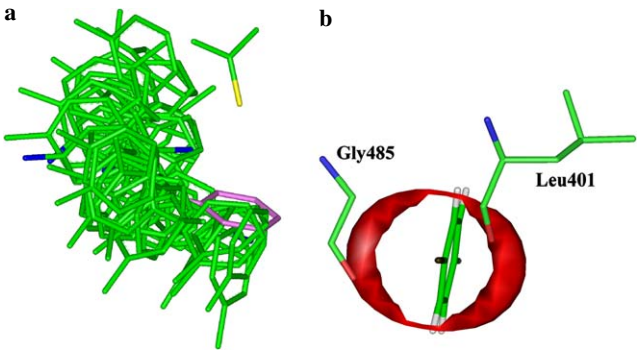

Figure 5. (a) CS-phenyl interactions observed in the CSD databank. The pink phenyl interacts with the thioxo group by CS…π bond; (b) Mep map of a Phe-Br (−10 kcal/mol), mimicking the one of compound **5**, facing Gly485 and Leu401 of the active site of FAAH.

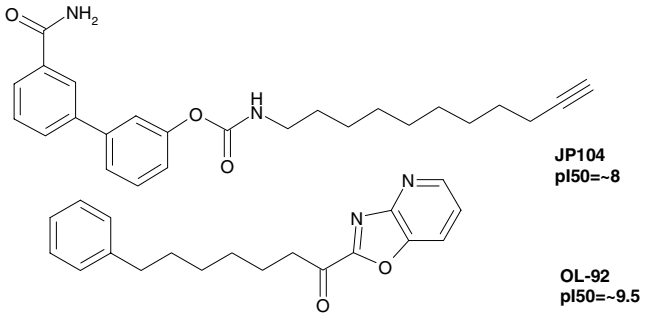

Figure 6. Molecular structure of two reference FAAH inhibitors: JP104 and OL-92, an irreversible and a reversible inhibitor, respectively.

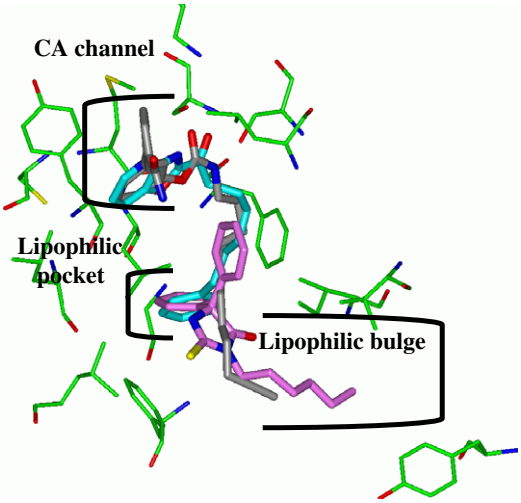

Figure 7. Proposed binding mode of JP104 (gray) and OL-92 (blue), superimposed to **1** (magenta), in the active site of rFAAH.

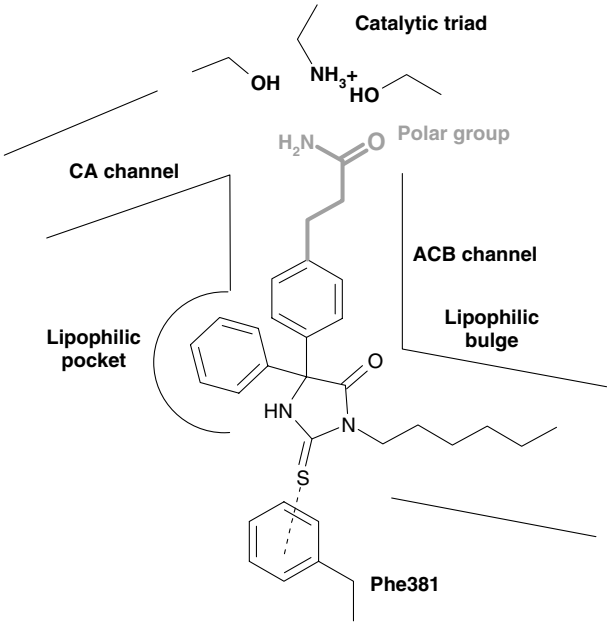

Figure 8. Structural modifications proposed to enhance the activity of **1** on FAAH.

The proposed molecule (Fig. 8) was docked in rFAAH and shows a better interaction energy than **1** (−39.8. kcal/mol), due to additional H bonds.

In conclusion, binding mode of new potential (thio)hydantoin inhibitors of FAAH was analyzed with the help of crystallography and docking studies. The alkyl chain binds to the ACB and one of the phenyl rings points toward the catalytic triad. The other phenyl group fills a lipophilic pocket often unoccupied by other reference inhibitors. The present model is in accordance with reported SAR of the series and will help to design more active compounds.

Acknowledgments

Catherine Michaux is grateful to FNRS for financial support. The work was also supported by a FRFC Grant (No. 2.4654.06).

References and notes

1. Ueda, N.; Kurahashi, Y.; Yamamoto, S.; Tokunaga, T. *J. Biol. Chem.* **1995**, *270*, 23823.
2. Cravatt, B. F.; Giang, D. K.; Mayfield, S. P.; Boger, D. L.; Lerner, R. A.; Gilula, N. B. *Nature* **1996**, *384*, 83.
3. Di Marzo, V.; Bisogno, T.; Sugiura, T.; Melck, D.; De Petrocellis, L. *Biochem. J.* **1998**, *331*, 15.
4. Bracey, M. H.; Hanson, M. A.; Masuda, K. R.; Stevens, R. C.; Cravatt, B. F. *Science* **2002**, *298*, 1793.
5. Patricelli, M. P.; Lovato, M. A.; Cravatt, B. F. *Biochemistry* **1999**, *38*, 9804.
6. Patricelli, M. P.; Cravatt, B. F. *J. Biol. Chem.* **2000**, *275*, 19177.
7. Martin, B. R.; Mechoulam, R.; Razdan, R. K. *Life Sci.* **1999**, *65*, 573.
8. Di Marzo, V.; Bisogno, T.; De Petrocellis, L.; Melck, D.; Martin, B. R. *Curr. Med. Chem.* **1999**, *6*, 721.
9. Axelrod, J.; Felder, C. C. *Neurochem. Res.* **1998**, *23*, 575.
10. Cravatt, B. F.; Lichtman, A. H. *Curr. Opin. Chem. Biol.* **2003**, *7*, 469.
11. Vandevoorde, S.; Lambert, D. M. *Curr. Pharm. Design* **2005**, *11*, 2647.
12. Boger, D. L.; Sato, H.; Lerner, A. E.; Austin, B. J.; Patterson, J. E.; Patricelli, M. P.; Cravatt, B. F. *Bioorg. Med. Chem. Lett.* **1999**, *9*, 265.
13. Deutsch, D. G.; Lin, S.; Hill, W. A. G.; Morse, K. L.; Salehani, D.; Arreaza, G.; Omeir, R. L.; Makriyannis, A. *Biochem. Biophys. Res. Commun.* **1997**, *231*, 217.
14. Deutsch, D. G.; Omeir, R.; Arreaza, G.; Salehani, D.; Prestwich, G. D.; Huang, Z.; Howlett, A. *Biochem. Pharmacol.* **1997**, *53*, 255.
15. Mor, M.; Rivara, S.; Lodola, A.; Plazzi, P. V.; Tarzia, G.; Duranti, A.; Tontini, A.; Piersanti, G.; Kathuria, S.; Piomelli, D. *J. Med. Chem.* **2004**, *47*, 4998.
16. Alexander, J. P.; Cravatt, B. F. *Chem. Biol.* **2005**, *12*, 1179.
17. Boger, D. L.; Miyauchi, H.; Du, W.; Hardouin, C.; Fecik, R. A.; Cheng, H.; Hwang, I.; Hedrick, M. P.; Leung, D.; Acevedo, O.; Guimaraes, C. R. W.; Jorgensen, W. L.; Cravatt, B. J. *J. Med. Chem.* **2005**, *48*, 1849.
18. Muccioli, G. G.; Fazio, N.; Scriba, G. K. E.; Poppitz, W.; Cannata, F.; Poupaert, J. H.; Wouters, J.; Lambert, D. M. *J. Med. Chem.* **2006**, *49*, 417.
19. Crystallographic data (excluding structure factors) for the structures in this paper have been deposited with the Cambridge Crystallographic Data Centre as supplementary publication numbers CCDC 606773.
20. Bruno, I. J.; Cole, J. C.; Lommerse, J. P.; Rowland, R. S.; Taylor, R.; Verdonk, M. L. *J. Comput. Aided Mol. Des.* **1997**, *11*, 525.
21. Sheldrick, G. *Shelxl97*; University of Göttingen: Germany, 1997.
22. Jones, G.; Willett, P.; Glen, R. C.; Leach, A. R.; Taylor, R. *J. Mol. Biol.* **1997**, *267*, 727.
23. Kellenberger, E.; Rodrigo, J.; Muller, P.; Rognan, D. *Proteins* **2004**, *57*, 225.
24. Discover3. 2.98 ed.; Accelrys Inc.: San Diego, CA.
25. InsightII; Accelrys Inc.: San Diego, CA, 2000.
26. Gaussian98. A.11 ed.; Gaussian Inc.: Pittsburgh, 2001. *X-ray studies.* Crystals of compound **1** were prepared by growth under slow evaporation at room temperature of

ethanol solution. Data were collected with a CAD4 Nonius diffractometer. The structure was solved using direct methods and refined with the Shelxl97 program.[21]

Molecular modeling. All computational experiments were conducted on a Silicon Graphics Octane2, running under IRIX 6.5 operating system. Docking studies were carried out using the genetic algorithm GOLD, performing automatic docking of flexible ligands into proteins with partial flexibility (Ser, Thr, Tyr, and Lys).[22] Default settings were used. GOLD is reported to have a good docking accuracy.[23] To take protein flexibility into account, the DISCOVER3 program,[24] from InsightII software,[25] was used to refine the complexes (CVFF forcefield and dielectric constant = 1∗r). Two steps of energy minimization were applied: the Steepest Descent algorithm (convergence: 10 kcal $mol^{-1\ -1}$) followed by the Conjugate Gradient algorithm (convergence: 0.01 kcal $mol^{-1\ -1}$). Quantum mechanics calculations were performed ab initio using 6–31 g* basis set (GAUSSIAN98 program).[26]